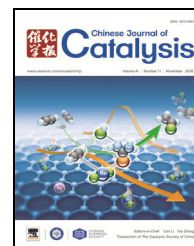


available at www.sciencedirect.comjournal homepage: www.elsevier.com/locate/chnjc

Article

Rhodium(III)-catalyzed chelation-assisted C–H imidation of arenes via umpolung of the imidating reagent

Guangfan Zheng ^{a,c}, Jiaqiong Sun ^a, Youwei Xu ^c, Xukai Zhou ^a, Hui Gao ^{b,#}, Xingwei Li ^{a,c,*}^a Key Laboratory of Applied Surface and Colloid Chemistry of MOE & School of Chemistry and Chemical Engineering Shaanxi Normal University (SNNU), Xi'an 710062, Shaanxi, China^b Key Laboratory of Molecular Target and Clinical Pharmacology, School of Pharmaceutical Sciences & Fifth Affiliated Hospital, Guangzhou Medical University, Guangzhou 511436, Guangdong, China^c Dalian Institute of Chemical Physics, Chinese Academy of Sciences, Dalian 116023, Liaoning, China

ARTICLE INFO

Article history:

Received 27 February 2020

Accepted 30 March 2020

Published 5 November 2020

Keywords:

Aryl amines

Rh(III) catalysis

Oxidative C–H imidation

Hypervalent iodine reagent

Umpolung

ABSTRACT

Rh(III)-catalyzed, chelation-assisted oxidative C–H imidation of arenes with N–H imide have been realized using $\text{PhI}(\text{OAc})_2$ as an oxidant. This transformation exhibits a broad substrate scope and tolerates various functional groups. The reaction proceeded via in situ generation of an iodine(III) imido. DFT calculations suggest that this oxidative imidation system proceeds via a Rh(III)-Rh(V)-Rh(III) pathway.

© 2020, Dalian Institute of Chemical Physics, Chinese Academy of Sciences.

Published by Elsevier B.V. All rights reserved.

1. Introduction

Aryl amines are a ubiquitous structural motif in pharmaceuticals, agrochemicals, and bioactive natural products [1–5]. Consequently, efficient synthetic procedures to access aryl amines has been actively investigated [6–9], such as Buchwald-Hartwig coupling [10,11], Chan-Lam amination [12,13], and the Ullmann reaction [14–17]. Owing to the accessibility of starting material and high atom/step-economy, transition metal-catalyzed direct C–H activation and amination of arenes has proved to be an advantageous strategy. Thus, Cu- [18–20], Pd- [21–23], Ru- [24,25], Co- [26], and Rh/Ir- catalyzed C–N formation reactions have been developed rapidly to access struc-

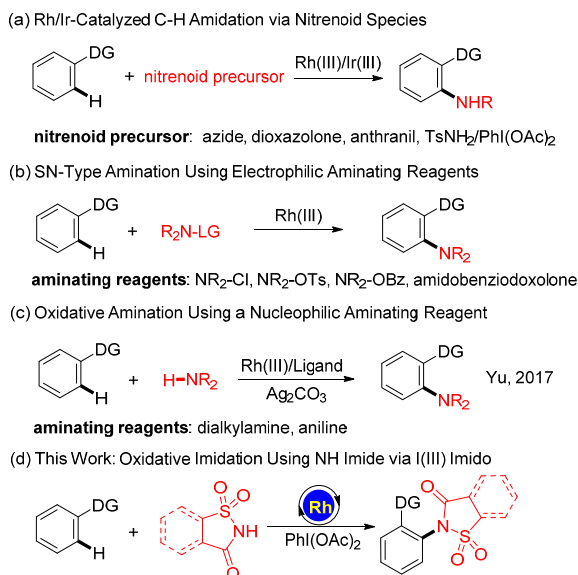
turally diverse aryl amines [18–31].

Among the numerous C–H activation catalysts, $\text{Cp}^*\text{Rh(III)/Ir(III)}$ complexes have stood out as competent catalysts for directing group-assisted direct C–H functionalization with high catalytic activity, selectivity, and functional group tolerance [32–39]. So far, the Rh(III)-catalyzed C–H amination proceeded via chelation-assisted strategies [34–70] include the following categories on the basis of the distinct mechanism: (1) the nitrene insertion using nitrene precursors such as organic azides, dioxazolones, anthranils, and $\text{TsNH}_2/\text{PhI}(\text{OAc})_2$ (Scheme 1(a)) [34–48,61,68,69], (2) S_N -type amination using an electrophilic aminating reagent (Scheme 1b) [49–60] and (3) the oxidative amination using a nucleophilic aminating re-

* Corresponding author. Tel: +86-029-85318783; E-mail: lixw@snnu.edu.cn# Corresponding author. E-mail: gaoh9@gzhmu.edu.cn

We acknowledge financial support from NSFC (21525208), China Postdoctoral Science Foundation (2019TQ0192, 2019M653531, 2019M663613), and Fundamental Research Funds for the Central Universities (GK201903028) and SNNU.

DOI: 10.1016/S1872-2067(20)63587-2 | <http://www.sciencedirect.com/science/journal/18722067> | Chin. J. Catal., Vol. 41, No. 11, November 2020



Scheme 1. Rh(III)-catalyzed chelation assisted C–H amination of arenes.

agent (Scheme 1(c)) [70]. Although amination has been realized under redox-neutral conditions using nitrenoid reagents [40–54] or electrophilic aminating reagents (*N*-halogen [55–58] and *N*-O [59–62] reagents, nitrosobenzenes [63,64], and amidobenziodoxolone [65,66]), they all rely on preactivation of a nucleophilic amine source. Thus, it will be desirable to directly employ nucleophilic amines for C–N coupling. Recently, Su et al. [67] and Chang et al. [68,69] realized Rh/Ir-catalyzed C–H imidation using TsNH₂ as an efficient nitrenoid precursor. Yu and co-workers [70] developed the first Rh(III)-catalyzed direct oxidative C–H amination of arenes using a secondary amine, leading to complementary tertiary amine products. However, a stoichiometric amount of Ag₂CO₃ was used. We reasoned that in-situ generation of highly electrophilic aminating reagent could be an alternative strategy for synthesis of tertiary amines. Hypervalent iodine(III) reagents with their high oxidation potential are a promising concept for oxidative amination owing to their environmental benignness and practicability [68,71–78]. Inspired by the chemistry of iodine(III) imido in C–N formation [71–78], we now report direct imidation of arenes via umpolung of NH saccharin.

2. Experimental

2.1. General information

Unless otherwise noted, all the coupling reactions were carried out in flame-dried pressure tubes with a Teflon screw cap under nitrogen atmosphere. Anhydrous solvents were purified and dried by standard procedures. All chemicals were obtained from commercial sources and were used as received unless otherwise noted. Oximes [79], arenes [80–82], saccharin derivatives [83] are prepared by following literature reports. ¹H and ¹³C NMR spectra were recorded on a Bruker AV 400 spectrometer (400 or 600 MHz for ¹H, 100 or 150 MHz for ¹³C). All cou-

pling constants were reported in Hz. The residual solvent signals were used as references for ¹H and ¹³C NMR spectra and the chemical shifts were converted to the TMS scale [CDCl₃: δ ¹H = 7.26 ppm, δ ¹³C = 77.16 ppm]. HRMS data were obtained using a TOF mode. Column chromatography was performed on silica gel (300–400 mesh) using ethyl acetate (EA)/petroleum ether (PE).

2.2. General procedure for synthesis of product 3

O-Me Oximes (**1**, 0.2 mmol), **2a** (0.3 mmol), PhI(OAc)₂ (0.3 mmol), RhCp*(CH₃CN)₃(SbF₆)₂ (5 mol%), and TFE (2.0 mL) were charged into a pressure tube. The reaction mixture was stirred at 100 °C for 48 h. After the solvent was removed under reduced pressure, the residue was purified by silica gel chromatography using PE/EA (3:1) to afford compound **3**.

2.3. General procedure for synthesis of product 5 or 6

Arenes (**1/4**, 0.2 mmol), **2** (0.3 mmol), PhI(OAc)₂ (0.3 mmol), [Cp*RhCl₂]₂ (4 mol%), NaOAc (0.06 mmol), and TFE (1.0 mL), CH₃CN (1.0 mL) were charged into a pressure tube. The reaction mixture was stirred at 100 °C for 48 h. After the solvent was removed under reduced pressure, the residue was purified by silica gel chromatography using PE/EA (2:1) to afford compound **5/6**.

2.4. Spectral data for products

3a. White solid. 53.5 mg, 81%. NMR Spectroscopy: ¹H NMR (600 MHz, CDCl₃) δ 8.16 (d, *J* = 7.4 Hz, 1H), 7.98 (d, *J* = 7.5 Hz, 1H), 7.91 (dt, *J* = 7.8, 1.2 Hz, 1H), 7.87 (dt, *J* = 7.8, 1.2 Hz, 1H), 7.61–7.50 (m, 4H), 3.53 (s, 3H), 2.16 (s, 3H). ¹³C NMR (150 MHz, CDCl₃) δ 158.9, 153.0, 138.1, 138.0, 134.9, 134.3, 131.7, 130.8, 130.0, 129.8, 127.3, 125.5, 125.4, 121.2, 61.5, 14.7. Mass Spectrometry: HRMS (ESI-TOF) (*m/z*): Calcd. for C₁₆H₁₅N₂O₄S⁺ ([M + H]⁺), 331.0747, found, 331.0750.

3b. White solid. 51.8 mg, 75%. NMR Spectroscopy: ¹H NMR (400 MHz, CDCl₃) δ 8.15 (dd, *J* = 7.2, 1.2 Hz, 1H), 8.01–7.92 (m, 1H), 7.92–7.83 (m, 2H), 7.64–7.48 (m, 4H), 3.49 (s, 3H), 2.67 (bs, 2H), 1.11 (t, *J* = 7.8 Hz, 3H). ¹³C NMR (100 MHz, CDCl₃) δ 158.9, 157.5, 138.0, 136.9, 134.8, 134.2, 132.0, 130.7, 129.9, 129.7, 127.4, 125.7, 125.4, 121.2, 61.4, 21.7, 10.6. Mass Spectrometry: HRMS (ESI-TOF) (*m/z*): Calcd. for C₁₇H₁₇N₂O₄S⁺ ([M + H]⁺), 345.0904, found, 345.0897.

3c. White solid. 54.9 mg, 77%. NMR Spectroscopy: ¹H NMR (400 MHz, CDCl₃) δ 8.19–8.12 (m, 1H), 7.97 (d, *J* = 7.2, 1.2 Hz, 1H), 7.90–7.85 (m, 2H), 7.60–7.51 (m, 4H), 3.50 (s, 3H), 2.61 (s, 2H), 1.60–1.52 (m, 2H), 0.93 (t, *J* = 7.2 Hz, 3H). ¹³C NMR (100 MHz, CDCl₃) δ 158.9, 156.6, 138.1, 137.1, 134.8, 134.2, 132.0, 130.7, 130.1, 129.7, 127.4, 125.7, 125.4, 121.2, 61.4, 30.5, 19.6, 14.4. Mass Spectrometry: HRMS (ESI-TOF) (*m/z*): Calcd. for C₁₈H₁₉N₂O₄S⁺ ([M + H]⁺), 359.1610, found, 359.1618.

3d. White solid. 63.1 mg, 80%. NMR Spectroscopy: ¹H NMR (400 MHz, CDCl₃) δ 8.04 (d, *J* = 7.4 Hz, 1H), 7.94 (d, *J* = 7.5 Hz, 1H), 7.83 (dt, *J* = 21.5, 7.1 Hz, 2H), 7.61–7.46 (m, 3H), 7.40–7.35 (m, 3H), 7.33–7.26 (m, 3H), 3.52 (s, 3H). ¹³C NMR (100 MHz,

CDCl₃) δ 158.5, 154.0, 137.9, 137.4, 134.7, 134.1, 132.8, 132.5, 131.9, 130.5, 130.1, 129.5, 128.9, 127.8, 127.3, 126.2, 125.3, 121.1, 62.0. Mass Spectrometry: HRMS (ESI-TOF) (m/z): Calcd. for C₂₁H₁₇N₂O₄S⁺ ([M + H]⁺), 393.0904, found, 393.0901.

3e. White solid. 59.2 mg, 86%. NMR Spectroscopy: ¹H NMR (400 MHz, CDCl₃) δ 8.20–8.12 (m, 1H), 7.97 (d, J = 7.1 Hz, 1H), 7.93–7.82 (m, 2H), 7.48 (d, J = 7.9 Hz, 1H), 7.41–7.34 (m, 2H), 3.48 (s, 3H), 2.43 (s, 3H), 2.14 (s, 3H). ¹³C NMR (100 MHz, CDCl₃) δ 159.0, 152.9, 140.2, 138.0, 134.9, 134.8, 134.2, 132.1, 131.5, 129.8, 127.4, 125.4, 125.0, 121.2, 61.4, 20.9, 14.6. Mass Spectrometry: HRMS (ESI-TOF) (m/z): Calcd. for C₁₇H₁₇N₂O₄S⁺ ([M + H]⁺), 345.0904, found, 345.0901.

3f. White solid. 59.4 mg, 80%. NMR Spectroscopy: ¹H NMR (400 MHz, CDCl₃) δ 8.16 (d, J = 7.0 Hz, 1H), 7.99 (d, J = 7.1 Hz, 1H), 7.91–7.87 (m, 2H), 7.51 (d, J = 8.1 Hz, 1H), 7.44 (dd, J = 8.1, 1.7 Hz, 1H), 7.38 (d, J = 1.7 Hz, 1H), 3.50 (s, 3H), 3.10–2.93 (m, 1H), 2.14 (s, 3H), 1.26 (d, J = 6.9 Hz, 6H). ¹³C NMR (100 MHz, CDCl₃) δ 159.0, 153.1, 151.1, 138.0, 135.2, 134.8, 134.2, 129.9, 129.8, 128.8, 127.4, 125.5, 125.1, 121.2, 61.5, 33.7, 23.6, 14.7. Mass Spectrometry: HRMS (ESI-TOF) (m/z): Calcd. for C₁₉H₂₁N₂O₄S⁺ ([M + H]⁺), 373.1217, found, 373.1225.

3g. White solid. 68.3 mg, 84%. NMR Spectroscopy: ¹H NMR (400 MHz, CDCl₃) δ 8.18 (d, J = 7.0 Hz, 1H), 8.00 (d, J = 7.2 Hz, 1H), 7.94–7.86 (m, 2H), 7.82–7.74 (m, 2H), 7.67–7.62 (m, 3H), 7.46 (t, J = 7.4 Hz, 2H), 7.40 (d, J = 7.2 Hz, 1H), 3.53 (s, 3H), 2.19 (s, 3H). ¹³C NMR (100 MHz, CDCl₃) δ 158.9, 152.8, 143.0, 138.9, 138.1, 136.3, 134.9, 134.3, 130.4, 130.3, 129.2, 129.0, 128.2, 127.4, 127.2, 125.8, 125.5, 121.3, 61.6, 14.6. Mass Spectrometry: HRMS (ESI-TOF) (m/z): Calcd. for C₂₂H₁₉N₂O₄S⁺ ([M + H]⁺), 407.1060, found, 407.1062.

3h. White solid. 63.9 mg, 89%. NMR Spectroscopy: ¹H NMR (400 MHz, CDCl₃) δ 8.15 (d, J = 7.1 Hz, 1H), 7.97 (d, J = 7.3 Hz, 1H), 7.92–7.82 (m, 2H), 7.50 (d, J = 8.6 Hz, 1H), 7.13–7.03 (m, 2H), 3.85 (s, 3H), 3.47 (s, 3H), 2.12 (s, 3H). ¹³C NMR (100 MHz, CDCl₃) δ 160.3, 158.9, 152.8, 138.1, 134.9, 134.3, 130.9, 130.1, 127.4, 126.4, 125.6, 121.3, 116.8, 116.6, 61.4, 55.7, 14.7. Mass Spectrometry: HRMS (ESI-TOF) (m/z): Calcd. for C₁₇H₁₇N₂O₅S⁺ ([M + H]⁺), 361.0853, found, 361.0861.

3i. White solid. 33.6 mg, 48%. NMR Spectroscopy: ¹H NMR (400 MHz, CDCl₃) δ 8.17 (d, J = 7.1 Hz, 1H), 7.99 (d, J = 7.2 Hz, 1H), 7.96–7.86 (m, 2H), 7.58 (dd, J = 8.5, 5.9 Hz, 1H), 7.37–7.27 (m, 2H), 3.53 (s, 3H), 2.14 (s, 3H). ¹³C NMR (100 MHz, CDCl₃) δ 162.4 (d, J = 252.3), 158.6, 152.4, 138.0, 135.1, 134.5, 134.4 (d, J = 4.0 Hz), 131.4 (d, J = 9.0 Hz), 127.2, 126.9 (d, J = 10.2 Hz), 125.7, 121.4, 119.0 (d, J = 23.4 Hz), 117.9 (d, J = 21.0 Hz), 61.6, 14.8. Mass Spectrometry: HRMS (ESI-TOF) (m/z): Calcd. for C₁₆H₁₄FN₂O₄S⁺ ([M + H]⁺), 349.0653, found, 349.0646.

3j. White solid. 62.1 mg, 86%. NMR Spectroscopy: ¹H NMR (400 MHz, CDCl₃) δ 8.17 (d, J = 7.1 Hz, 1H), 8.06–7.82 (m, 3H), 7.66–7.45 (m, 3H), 3.52 (s, 3H), 2.13 (s, 3H). ¹³C NMR (100 MHz, CDCl₃) δ 158.7, 152.3, 138.0, 136.5, 135.2, 135.1, 134.5, 131.7, 131.0, 131.0, 127.2, 126.6, 125.7, 121.4, 61.7, 14.6. Mass Spectrometry: HRMS (ESI-TOF) (m/z): Calcd. for C₁₆H₁₄ClN₂O₄S⁺ ([M + H]⁺), 365.0357, found, 365.0343.

3k. White solid. 59.5 mg, 77%. NMR Spectroscopy: ¹H NMR (400 MHz, CDCl₃) δ 8.31–8.14 (m, 3H), 8.00 (d, J = 7.4 Hz, 1H), 7.97–7.85 (m, 2H), 7.68 (d, J = 8.1 Hz, 1H), 3.94 (s, 3H), 3.55 (s,

3H), 2.17 (s, 3H). ¹³C NMR (100 MHz, CDCl₃) δ 165.3, 158.9, 152.5, 142.2, 138.1, 135.1, 134.4, 133.1, 131.8, 131.6, 130.2, 127.2, 125.8, 125.6, 121.4, 61.8, 52.5, 14.6. Mass Spectrometry: HRMS (ESI-TOF) (m/z): Calcd. for C₁₈H₁₇N₂O₆S⁺ ([M + H]⁺), 389.0802, found, 389.0801.

3l. White solid. 52.3 mg, 64%. NMR Spectroscopy: ¹H NMR (400 MHz, CDCl₃) δ 8.16 (d, J = 7.2 Hz, 1H), 7.98 (d, J = 7.1 Hz, 1H), 7.96–7.82 (m, 2H), 7.73 (d, J = 2.2 Hz, 1H), 7.65 (dd, J = 8.4, 2.2 Hz, 1H), 7.42 (d, J = 8.4 Hz, 1H), 3.56 (s, 3H), 2.13 (s, 3H). ¹³C NMR (100 MHz, CDCl₃) δ 158.7, 152.0, 139.8, 138.1, 135.1, 134.4, 133.2, 133.0, 132.9, 127.2, 125.6, 125.2, 124.6, 121.4, 61.8, 14.6. Mass Spectrometry: HRMS (ESI-TOF) (m/z): Calcd. for C₁₆H₁₄BrN₂O₄S⁺ ([M + H]⁺), 408.9852, found, 408.9847.

3m. White solid. 56.3 mg, 82%. NMR Spectroscopy: ¹H NMR (400 MHz, CDCl₃) δ 8.14 (d, J = 7.1 Hz, 1H), 7.96 (d, J = 7.1 Hz, 1H), 7.92–7.82 (m, 2H), 7.42 (d, J = 8.0 Hz, 1H), 7.39 (s, 1H), 7.32 (d, J = 8.0 Hz, 1H), 3.55 (s, 3H), 2.44 (s, 3H), 2.14 (s, 3H). ¹³C NMR (100 MHz, CDCl₃) δ 158.9, 153.2, 141.2, 138.0, 137.7, 134.8, 134.2, 131.4, 130.7, 130.4, 127.3, 125.4, 122.6, 121.2, 61.5, 21.3. Mass Spectrometry: HRMS (ESI-TOF) (m/z): Calcd. for C₁₇H₁₇N₂O₄S⁺ ([M + H]⁺), 345.0904, found, 345.0911.

3n. White solid. 62.9 mg, 87%. NMR Spectroscopy: ¹H NMR (400 MHz, CDCl₃) δ 8.14 (d, J = 7.2 Hz, 1H), 7.96 (d, J = 7.7 Hz, 1H), 7.92–7.82 (m, 2H), 7.44 (d, J = 8.7 Hz, 1H), 7.08 (d, J = 2.8 Hz, 1H), 7.01 (dd, J = 8.7, 2.9 Hz, 1H), 3.86 (s, 3H), 3.55 (s, 3H), 2.14 (s, 3H). ¹³C NMR (100 MHz, CDCl₃) δ 161.2, 159.1, 153.0, 139.4, 138.0, 134.9, 134.3, 133.1, 127.4, 125.5, 121.3, 117.4, 116.0, 114.7, 61.6, 55.7, 14.8. Mass Spectrometry: HRMS (ESI-TOF) (m/z): Calcd. for C₁₇H₁₇N₂O₅S⁺ ([M + H]⁺), 361.0853, found, 361.0846.

3o. White solid. 40.5 mg, 58%. NMR Spectroscopy: ¹H NMR (400 MHz, CDCl₃) δ 8.16 (d, J = 7.1 Hz, 1H), 7.99 (d, J = 7.2 Hz, 1H), 7.95–7.86 (m, 2H), 7.51 (td, J = 8.2, 5.9 Hz, 1H), 7.39 (d, J = 7.9 Hz, 1H), 7.35–7.29 (m, 1H), 3.56 (s, 3H), 2.16 (d, J = 2.3 Hz, 3H). ¹³C NMR (100 MHz, CDCl₃) δ 161.5 (d, J = 250.8 Hz), 158.7, 149.9, 137.9, 135.1, 134.5, 130.6 (d, J = 9.7 Hz), 127.4 (d, J = 5.8 Hz), 127.2 (d, J = 3.3 Hz), 127.0, 125.6, 121.4, 118.7 (d, J = 22.2 Hz), 61.8, 15.9 (d, J = 4.0 Hz). Mass Spectrometry: HRMS (ESI-TOF) (m/z): Calcd. for C₁₆H₁₄FN₂O₄S⁺ ([M + H]⁺), 349.0653, found, 349.0660.

3p. White solid. 58.1 mg, 81%. NMR Spectroscopy: ¹H NMR (400 MHz, CDCl₃) δ 8.13 (d, J = 7.6 Hz, 1H), 7.96 (d, J = 7.2 Hz, 1H), 7.93–7.82 (m, 2H), 7.47 (t, J = 8.2 Hz, 1H), 7.16 (d, J = 7.9 Hz, 1H), 7.11 (d, J = 8.4 Hz, 1H), 3.86 (s, 3H), 3.59 (s, 3H), 2.12 (s, 3H). ¹³C NMR (100 MHz, CDCl₃) δ 158.9, 158.7, 152.3, 137.8, 134.8, 134.2, 130.3, 128.1, 127.1, 126.9, 125.4, 122.9, 121.2, 113.4, 61.4, 55.9, 16.0. Mass Spectrometry: HRMS (ESI-TOF) (m/z): Calcd. for C₁₇H₁₇N₂O₅S⁺ ([M + H]⁺), 361.0853, found, 361.0862.

3q. White solid. 61.0 mg, 85%. NMR Spectroscopy: ¹H NMR (400 MHz, CDCl₃) δ 8.19–8.12 (m, 1H), 7.97 (d, J = 7.1 Hz, 1H), 7.93–7.81 (m, 2H), 7.35 (s, 1H), 7.29 (s, 1H), 3.51 (s, 3H), 2.33 (s, 3H), 2.32 (s, 3H), 2.13 (s, 3H). ¹³C NMR (100 MHz, CDCl₃) δ 159.0, 153.1, 139.8, 138.8, 138.1, 135.1, 134.7, 134.2, 132.4, 131.1, 127.4, 125.4, 122.4, 121.2, 61.4, 19.7, 19.5, 14.7. Mass Spectrometry: HRMS (ESI-TOF) (m/z): Calcd. for C₁₈H₁₉N₂O₄S⁺ ([M + H]⁺), 359.1060, found, 359.1059.

3r. White solid. 59.1 mg, 78%. NMR Spectroscopy: ^1H NMR (400 MHz, CDCl_3) δ 8.17 (dd, $J = 6.8, 1.2$ Hz, 1H), 8.09 (s, 1H), 8.05 (s, 1H), 7.99 (dd, $J = 6.9, 1.0$ Hz, 1H), 7.94 – 7.81 (m, 4H), 7.65–7.54 (m, 2H), 3.48 (s, 3H), 2.27 (s, 3H). ^{13}C NMR (100 MHz, CDCl_3) δ 159.2, 153.1, 138.1, 134.8, 134.2, 133.8, 133.6, 132.8, 131.9, 130.1, 128.2, 128.1, 128.0, 127.6, 127.5, 125.5, 122.9, 121.2, 61.4, 14.78. Mass Spectrometry: HRMS (ESI-TOF) (m/z): Calcd. for $\text{C}_{20}\text{H}_{17}\text{N}_2\text{O}_4\text{S}^+$ ($[\text{M} + \text{H}]^+$), 381.0904, found, 381.0912.

3s. White solid. 51.3 mg, 76%. NMR Spectroscopy: ^1H NMR (400 MHz, CDCl_3) δ 8.16 (d, $J = 7.3$ Hz, 1H), 7.99 (d, $J = 7.4$ Hz, 1H), 7.96–7.82 (m, 2H), 7.41 (d, $J = 5.3$ Hz, 1H), 7.18 (d, $J = 5.3$ Hz, 1H), 3.66 (s, 3H), 2.15 (s, 3H). ^{13}C NMR (100 MHz, CDCl_3) δ 158.3, 148.5, 139.5, 138.2, 135.1, 134.4, 128.7, 127.3, 125.6, 125.3, 121.3, 121.2, 62.0, 13.8. Mass Spectrometry: HRMS (ESI-TOF) (m/z): Calcd. for $\text{C}_{14}\text{H}_{13}\text{N}_2\text{O}_4\text{S}_2^+$ ($[\text{M} + \text{H}]^+$), 337.0311, found, 337.0315.

3t. White solid. 47.1 mg, 64%. NMR Spectroscopy: ^1H NMR (600 MHz, CDCl_3) δ 8.22 (d, $J = 7.5$ Hz, 1H), 8.05 (d, $J = 7.6$ Hz, 1H), 7.97 (t, $J = 7.5$ Hz, 1H), 7.93 (t, $J = 7.5$ Hz, 1H), 7.71 (d, $J = 7.7$ Hz, 1H), 7.60 (d, $J = 8.3$ Hz, 1H), 7.43 (t, $J = 7.7$ Hz, 1H), 7.36 (t, $J = 7.5$ Hz, 1H), 3.61 (s, 3H), 2.28 (s, 3H). ^{13}C NMR (150 MHz, CDCl_3) δ 158.2, 153.4, 149.8, 146.9, 138.4, 135.1, 134.5, 127.6, 126.5, 126.2, 125.6, 124.46, 121.25, 119.96, 112.02, 106.85, 62.35, 11.23. Mass Spectrometry: HRMS (ESI-TOF) (m/z): Calcd. for $\text{C}_{18}\text{H}_{14}\text{N}_2\text{NaO}_5\text{S}^+$ ($[\text{M} + \text{Na}]^+$), 393.0516, found, 361.0510.

3u. White solid. 52.1 mg, 73%. NMR Spectroscopy: ^1H NMR (400 MHz, CDCl_3) δ 8.16 (d, $J = 7.2$ Hz, 1H), 7.98 (d, $J = 7.4$ Hz, 1H), 7.92–7.85 (m, 2H), 7.37 (t, $J = 8.0$ Hz, 1H), 7.19 (d, $J = 7.5$ Hz, 1H), 7.12 (d, $J = 8.4$ Hz, 1H), 4.36–4.11 (m, 2H), 3.18 (s, 3H), 3.04–2.91 (m, 1H), 2.85–2.71 (m, 1H). ^{13}C NMR (100 MHz, CDCl_3) δ 159.0, 158.5, 146.6, 138.3, 134.6, 134.1, 130.4, 128.2, 125.4, 125.2, 124.6, 121.0, 120.9, 117.7, 64.7, 61.2, 23.6. Mass Spectrometry: HRMS (ESI-TOF) (m/z): Calcd. for $\text{C}_{17}\text{H}_{15}\text{N}_2\text{O}_5\text{S}^+$ ($[\text{M} + \text{H}]^+$), 359.0696, found, 359.0699.

5a. White solid. 58.4 mg, 87%. NMR Spectroscopy: ^1H NMR (400 MHz, CDCl_3) δ 8.48 (d, $J = 4.7$ Hz, 1H), 8.06 (d, $J = 7.1$ Hz, 1H), 7.92–7.81 (m, 4H), 7.71–7.55 (m, 5H), 7.15–7.12 (m, 1H). ^{13}C NMR (100 MHz, CDCl_3) δ 158.7, 156.3, 149.5, 141.1, 137.8, 136.4, 134.9, 134.3, 131.6, 131.2, 131.0, 129.9, 127.1, 126.0, 125.6, 123.0, 122.4, 121.2. Mass Spectrometry: HRMS (ESI-TOF) (m/z): Calcd. for $\text{C}_{18}\text{H}_{13}\text{N}_2\text{O}_3\text{S}^+$ ($[\text{M} + \text{H}]^+$), 337.0641, found, 337.0632.

5b. White solid. 65.2 mg, 93%. NMR Spectroscopy: ^1H NMR (400 MHz, CDCl_3) δ 8.44 (d, $J = 4.6$ Hz, 1H), 8.06 (d, $J = 7.0$ Hz, 1H), 7.91–7.80 (m, 3H), 7.72 (d, $J = 7.9$ Hz, 1H), 7.60–7.54 (m, 2H), 7.49–7.40 (m, 2H), 7.15–7.05 (m, 1H), 2.47 (s, 3H). ^{13}C NMR (100 MHz, CDCl_3) δ 158.9, 156.4, 149.4, 140.3, 138.0, 137.8, 136.3, 134.8, 134.3, 131.8, 131.6, 131.4, 127.2, 125.7, 125.5, 122.9, 122.2, 121.2, 21.1. Mass Spectrometry: HRMS (ESI-TOF) (m/z): Calcd. for $\text{C}_{19}\text{H}_{15}\text{N}_2\text{O}_3\text{S}^+$ ($[\text{M} + \text{H}]^+$), 351.0798, found, 351.0810.

5c. White solid. 62.6 mg, 71%. NMR Spectroscopy: ^1H NMR (400 MHz, CDCl_3) δ 8.42 (d, $J = 4.4$ Hz, 1H), 8.05 (d, $J = 7.0$ Hz, 1H), 7.92–7.80 (m, 3H), 7.76 (d, $J = 8.4$ Hz, 1H), 7.59–7.52 (m, 2H), 7.46 (d, $J = 7.0$ Hz, 2H), 7.41 (t, $J = 7.0$ Hz, 2H), 7.37 – 7.31 (m, 1H), 7.26–7.23 (m, 2H), 7.11–7.05 (m, 1H), 5.14 (s, 2H). ^{13}C

NMR (100 MHz, CDCl_3) δ 159.6, 158.6, 156.1, 149.3, 137.7, 136.3, 136.1, 134.8, 134.2, 133.4, 132.4, 128.6, 128.2, 127.6, 127.1, 126.8, 125.5, 122.6, 121.9, 121.2, 117.5, 116.9, 70.4. Mass Spectrometry: HRMS (ESI-TOF) (m/z): Calcd. for $\text{C}_{25}\text{H}_{19}\text{N}_2\text{O}_4\text{S}^+$ ($[\text{M} + \text{H}]^+$), 443.1060, found, 443.1053.

5d. White solid. 68.0 mg, 83%. NMR Spectroscopy: ^1H NMR (400 MHz, CDCl_3) δ 8.48 (d, $J = 4.7$ Hz, 1H), 8.06 (d, $J = 7.1$ Hz, 1H), 7.90–7.79 (m, 6H), 7.68–7.59 (m, 4H), 7.47 (t, $J = 7.5$ Hz, 2H), 7.39 (t, $J = 7.3$ Hz, 1H), 7.18–7.10 (m, 1H). ^{13}C NMR (100 MHz, CDCl_3) δ 158.8, 156.0, 149.6, 143.1, 139.5, 139.1, 137.9, 136.5, 134.9, 134.3, 132.0, 129.7, 129.5, 129.0, 128.2, 127.3, 127.2, 126.5, 125.6, 122.9, 122.4, 121.3. Mass Spectrometry: HRMS (ESI-TOF) (m/z): Calcd. for $\text{C}_{24}\text{H}_{17}\text{N}_2\text{O}_3\text{S}^+$ ($[\text{M} + \text{H}]^+$), 413.0954, found, 413.0957.

5e. White solid. 33.4 mg, 46%. NMR Spectroscopy: ^1H NMR (400 MHz, CDCl_3) δ 10.12 (s, 1H), 8.52 (d, $J = 4.7$ Hz, 1H), 8.23 – 8.12 (m, 2H), 8.08 (d, $J = 7.2$ Hz, 1H), 8.02 (d, $J = 8.0$ Hz, 1H), 7.96–7.84 (m, 3H), 7.66–7.63 (m, 2H), 7.22–7.18 (m, 1H). ^{13}C NMR (100 MHz, CDCl_3) δ 190.4, 158.6, 155.1, 149.8, 146.4, 137.8, 137.3, 136.7, 135.1, 134.5, 132.9, 132.6, 131.0, 127.2, 126.9, 125.7, 123.2, 121.4. Mass Spectrometry: HRMS (ESI-TOF) (m/z): Calcd. for $\text{C}_{19}\text{H}_{13}\text{N}_2\text{O}_4\text{S}^+$ ($[\text{M} + \text{H}]^+$), 365.0591, found, 365.0598.

5f. White solid. 40.6 mg, 52%. NMR Spectroscopy: ^1H NMR (400 MHz, CDCl_3) δ 8.50 (d, $J = 4.6$ Hz, 1H), 8.39–8.25 (m, 2H), 8.08 (d, $J = 7.0$ Hz, 1H), 7.95–7.81 (m, 4H), 7.71–7.56 (m, 2H), 7.19–7.16 (m, 1H), 3.96 (s, 3H). ^{13}C NMR (100 MHz, CDCl_3) δ 165.5, 158.7, 155.4, 149.7, 145.2, 137.8, 136.6, 135.0, 134.4, 132.7, 131.9, 131.8, 131.7, 127.0, 126.4, 125.6, 123.2, 123.0, 121.3, 52.6. Mass Spectrometry: HRMS (ESI-TOF) (m/z): Calcd. for $\text{C}_{20}\text{H}_{15}\text{N}_2\text{O}_5\text{S}^+$ ($[\text{M} + \text{H}]^+$), 395.0696, found, 395.0682.

5g. White solid. 54.0 mg, 76%. NMR Spectroscopy: ^1H NMR (400 MHz, CDCl_3) δ 8.48–8.47 (m, 1H), 8.05 (d, $J = 7.3$ Hz, 1H), 7.95–7.78 (m, 4H), 7.60–7.54 (m, 2H), 7.40 – 7.35 (m, 2H), 7.16–7.14 (m, 1H). ^{13}C NMR (100 MHz, CDCl_3) δ 162.6 (d, $J = 252.8$ Hz), 158.3, 155.4, 149.6, 137.7, 137.3 (d, $J = 3.7$ Hz), 136.5, 135.0, 134.4, 133.0 (d, $J = 9.0$ Hz), 127.2 (d, $J = 10.5$ Hz), 126.8, 125.6, 122.8, 122.4, 121.3, 118.3 (d, $J = 15.7$ Hz), 118.0 (d, $J = 12.9$ Hz). Mass Spectrometry: HRMS (ESI-TOF) (m/z): Calcd. for $\text{C}_{18}\text{H}_{12}\text{FN}_2\text{O}_3\text{S}^+$ ($[\text{M} + \text{H}]^+$), 355.0547, found, 355.0560.

5h. White solid. 43.1 mg, 58%. NMR Spectroscopy: ^1H NMR (400 MHz, CDCl_3) δ 8.47 (d, $J = 4.3$ Hz, 1H), 8.05 (d, $J = 7.2$ Hz, 1H), 7.93–7.88 (m, 2H), 7.86–7.82 (m, 1H), 7.78 (d, $J = 8.2$ Hz, 1H), 7.69–7.53 (m, 4H), 7.16–7.13 (m, 1H). ^{13}C NMR (100 MHz, CDCl_3) δ 158.4, 155.3, 149.6, 139.5, 137.8, 136.5, 135.3, 135.1, 134.4, 132.6, 131.2, 131.1, 127.1, 126.9, 125.7, 122.9, 122.6, 121.3. Mass Spectrometry: HRMS (ESI-TOF) (m/z): Calcd. for $\text{C}_{18}\text{H}_{12}\text{ClN}_2\text{O}_3\text{S}^+$ ($[\text{M} + \text{H}]^+$), 371.0252, found, 371.0249.

5i. White solid. 62.0 mg, 89%. NMR Spectroscopy: ^1H NMR (400 MHz, CDCl_3) δ 8.55–8.47 (m, 1H), 8.08–8.01 (m, 1H), 7.92–7.78 (m, 3H), 7.64 (d, $J = 1.6$ Hz, 1H), 7.62–7.54 (m, 2H), 7.50 (d, $J = 8.0$ Hz, 1H), 7.39 (dd, $J = 8.1, 1.5$ Hz, 1H), 7.14–7.11 (m, 1H), 2.49 (s, 3H). ^{13}C NMR (100 MHz, CDCl_3) δ 158.8, 156.4, 149.6, 141.4, 140.8, 137.8, 136.3, 134.8, 134.3, 132.3, 130.9, 130.6, 127.1, 125.5, 123.2, 122.9, 122.3, 121.2, 21.4. Mass Spectrometry: HRMS (ESI-TOF) (m/z): Calcd. for $\text{C}_{19}\text{H}_{15}\text{N}_2\text{O}_3\text{S}^+$ ($[\text{M} + \text{H}]^+$), 351.0798, found, 351.0807.

5j. White solid. 56.5 mg, 68%. NMR Spectroscopy: ^1H NMR (400 MHz, CDCl_3) δ 8.51 (d, $J = 4.5$ Hz, 1H), 8.05 (d, $J = 7.2$ Hz, 1H), 7.99 (d, $J = 2.3$ Hz, 1H), 7.92–7.88 (m, 2H), 7.83 (td, $J = 7.3$, 1.6 Hz, 1H), 7.71 (dd, $J = 8.4$, 2.3 Hz, 1H), 7.64–7.56 (m, 2H), 7.50 (d, $J = 8.4$ Hz, 1H), 7.20–7.13 (m, 1H). ^{13}C NMR (100 MHz, CDCl_3) δ 158.4, 155.3, 149.6, 139.5, 137.8, 136.5, 135.3, 135.1, 134.4, 132.6, 131.2, 131.1, 127.1, 126.9, 125.7, 122.9, 122.6, 121.3. Mass Spectrometry: HRMS (ESI-TOF) (m/z): Calcd. for $\text{C}_{18}\text{H}_{12}\text{BrN}_2\text{O}_3\text{S}^+$ ($[\text{M} + \text{H}]^+$), 414.9747, found, 414.9754.

5k. brown solid. 41.2 mg, 60%. NMR Spectroscopy: NMR Spectroscopy: ^1H NMR (400 MHz, CDCl_3) δ 8.49 (d, $J = 4.3$ Hz, 1H), 8.13 (d, $J = 7.4$ Hz, 1H), 8.01 (d, $J = 7.4$ Hz, 1H), 7.98–7.83 (m, 2H), 7.68–7.47 (m, 3H), 7.23 (d, $J = 5.3$ Hz, 1H), 7.17–7.10 (m, 1H). ^{13}C NMR (100 MHz, CDCl_3) δ 158.2, 150.3, 149.6, 143.9, 138.0, 136.9, 135.3, 134.6, 128.8, 127.1, 126.5, 125.8, 123.0, 121.5, 120.8, 120.4. Mass Spectrometry: HRMS (ESI-TOF) (m/z): Calcd. for $\text{C}_{16}\text{H}_{11}\text{N}_2\text{O}_3\text{S}_2^+$ ($[\text{M} + \text{H}]^+$), 343.0206, found, 343.0193.

5l. white solid. 48.4 mg, 65%. NMR Spectroscopy: ^1H NMR (400 MHz, CDCl_3) δ 8.47–8.41 (m, 1H), 8.10–8.05 (m, 1H), 7.95–7.82 (m, 3H), 7.79 (dd, $J = 7.5$, 1.1 Hz, 1H), 7.68–7.53 (m, 5H). ^{13}C NMR (100 MHz, CDCl_3) δ 158.6, 154.4, 148.4, 139.9, 137.8, 136.2, 135.0, 134.4, 131.5, 131.3, 131.13, 131.06, 130.2, 127.0, 126.0, 125.7, 123.8, 121.3. Mass Spectrometry: HRMS (ESI-TOF) (m/z): Calcd. for $\text{C}_{18}\text{H}_{12}\text{ClN}_2\text{O}_3\text{S}^+$ ($[\text{M} + \text{H}]^+$), 371.0252, found, 371.0249.

5m. Colorless oil. 56.7 mg, 74%. NMR Spectroscopy: ^1H NMR (400 MHz, CDCl_3) δ 8.15 (d, $J = 6.9$ Hz, 1H), 7.97 (d, $J = 7.2$ Hz, 1H), 7.92–7.82 (m, 2H), 7.68–7.49 (m, 4H), 4.58 (apparent s, 1H), 3.53–3.22 (m, 1H), 3.05–2.86 (m, 1H), 1.70 (apparent s, 1H), 1.57–1.45 (m, 1H), 1.29 (apparent s, 4H), 0.86 (apparent s, 3H). ^{13}C NMR (100 MHz, CDCl_3) δ 158.9, 153.5, 138.0, 134.9, 134.4, 132.4, 130.9, 130.6, 130.2, 127.5, 125.8, 125.6, 121.3, 81.1, 41.4, 34.6, 27.6, 22.5, 13.9. Mass Spectrometry: HRMS (ESI-TOF) (m/z): Calcd. for $\text{C}_{20}\text{H}_{21}\text{N}_2\text{O}_4\text{S}^+$ ($[\text{M} + \text{H}]^+$), 385.1217, found, 385.1221.

5n. White solid. 67.4 mg, 84%. NMR Spectroscopy: ^1H NMR (400 MHz, d_6 -DMSO) δ 8.43 (d, $J = 7.6$ Hz, 1H), 8.26 (d, $J = 7.3$ Hz, 1H), 8.21–8.07 (m, 3H), 7.93–7.81 (m, 4H), 7.81–7.76 (m, 1H), 7.61–7.50 (m, 4H). ^{13}C NMR (100 MHz, d_6 -DMSO) δ 169.5, 160.8, 158.9, 137.5, 136.5, 135.9, 132.8, 132.1, 132.0, 131.5, 131.1, 130.3, 129.8, 127.0, 126.9, 126.1, 126.0, 125.9, 122.5, 100.6. Mass Spectrometry: HRMS (ESI-TOF) (m/z): Calcd. for $\text{C}_{22}\text{H}_{15}\text{N}_2\text{O}_4\text{S}^+$ ($[\text{M} + \text{H}]^+$), 403.0747, found, 403.0752.

5o. White solid. 58.7 mg, 73%. NMR Spectroscopy: ^1H NMR (400 MHz, CDCl_3) δ 8.53 (d, $J = 8.0$ Hz, 1H), 8.50 (s, 1H), 8.18–8.11 (m, 1H), 8.04 (s, 1H), 7.87 (d, $J = 2.7$ Hz, 3H), 7.56 (d, $J = 8.0$ Hz, 1H), 7.52 (s, 1H), 3.86 (s, 3H), 2.52 (s, 3H). ^{13}C NMR (100 MHz, CDCl_3) δ 159.5, 154.3, 152.6, 151.5, 145.2, 142.2, 137.9, 134.7, 134.2, 133.8, 132.9, 131.8, 131.48, 131.45, 127.7, 126.6, 125.5, 121.1, 29.8, 21.3. Mass Spectrometry: HRMS (ESI-TOF) (m/z): Calcd. for $\text{C}_{20}\text{H}_{16}\text{N}_5\text{O}_3\text{S}^+$ ($[\text{M} + \text{H}]^+$), 406.0968, found, 406.0963.

5p. yellow oil. 50.8mg, 78%. NMR Spectroscopy: ^1H NMR (400 MHz, CDCl_3) δ 8.05 (d, $J = 7.4$ Hz, 1H), 7.96 (d, $J = 7.5$ Hz, 1H), 7.90 (t, $J = 7.5$ Hz, 1H), 7.86–7.82 (m, 2H), 7.75–7.63 (m, 3H), 7.58–7.52 (m, 2H), 6.33–6.27 (m, 1H). ^{13}C NMR (100 MHz,

CDCl_3) δ 156.0, 139.7, 137.8, 135.9, 133.2, 132.6, 129.8, 129.6, 128.0, 126.8, 125.0, 124.8, 123.8, 119.9, 119.9, 105.6. Mass Spectrometry: HRMS (ESI-TOF) (m/z): Calcd. for $\text{C}_{16}\text{H}_{12}\text{N}_3\text{O}_3\text{S}^+$ ($[\text{M} + \text{H}]^+$), 326.0594, found, 326.0585.

5q. White solid. 34.5 mg, 46%. NMR Spectroscopy: ^1H NMR (400 MHz, CDCl_3) δ 8.90 (d, $J = 8.5$ Hz, 1H), 8.73 (d, $J = 4.8$ Hz, 2H), 8.68 (s, 1H), 8.21 (d, $J = 7.2$ Hz, 1H), 8.04 (d, $J = 7.3$ Hz, 1H), 7.99–7.86 (m, 2H), 7.56 (d, $J = 7.9$ Hz, 1H), 7.43 (t, $J = 7.7$ Hz, 1H), 7.30 (t, $J = 7.5$ Hz, 1H), 7.13 (t, $J = 4.8$ Hz, 1H). ^{13}C NMR (100 MHz, CDCl_3) δ 158.5, 158.3, 157.3, 138.1, 135.1, 134.8, 134.5, 127.4, 127.2, 125.9, 125.7, 125.0, 123.2, 121.5, 118.6, 117.1, 116.9, 108.1. Mass Spectrometry: HRMS (ESI-TOF) (m/z): Calcd. for $\text{C}_{19}\text{H}_{13}\text{N}_4\text{O}_3\text{S}^+$ ($[\text{M} + \text{H}]^+$), 377.0703, found, 377.0706.

5r. White solid. 73.2 mg, 94%. NMR Spectroscopy: ^1H NMR (400 MHz, CDCl_3) δ 8.59 (d, $J = 8.5$ Hz, 1H), 8.41 (d, $J = 4.8$ Hz, 2H), 8.25–8.23 (m, 1H), 7.99–7.86 (m, 3H), 7.68 (d, $J = 7.8$ Hz, 1H), 7.48–7.40 (m, 1H), 7.32 (t, $J = 7.5$ Hz, 1H), 6.93 (t, $J = 4.8$ Hz, 1H), 2.45 (s, 3H). ^{13}C NMR (100 MHz, CDCl_3) δ 155.2, 153.0, 152.4, 133.5, 131.1, 130.4, 129.6, 123.4, 122.7, 121.1, 121.0, 117.5, 117.0, 116.7, 114.9, 112.7, 112.1, 111.0, 3.8. Mass Spectrometry: HRMS (ESI-TOF) (m/z): Calcd. for $\text{C}_{20}\text{H}_{15}\text{N}_4\text{O}_3\text{S}^+$ ($[\text{M} + \text{H}]^+$), 391.0859, found, 391.0848.

5s. White solid. 73.3 mg, 86%. NMR Spectroscopy: ^1H NMR (400 MHz, CDCl_3) δ 8.41 (d, $J = 4.8$ Hz, 2H), 8.30 (d, $J = 7.0$ Hz, 1H), 8.23 (d, $J = 8.3$ Hz, 1H), 7.14–7.10 (m, 2H), 7.93–7.76 (m, 3H), 7.58 (d, $J = 7.0$ Hz, 1H), 7.53 (d, $J = 7.6$ Hz, 1H), 7.46 (t, $J = 7.6$ Hz, 1H), 7.38 (t, $J = 7.4$ Hz, 1H), 6.81 (t, $J = 4.8$ Hz, 1H). ^{13}C NMR (100 MHz, CDCl_3) δ 158.2, 157.8, 157.4, 140.5, 137.4, 136.1, 134.2, 134.3, 130.1, 129.1, 127.5, 127.3, 125.0, 124.1, 122.5, 122.5, 122.4, 121.1, 119.8, 117.4, 113.4. Mass Spectrometry: HRMS (ESI-TOF) (m/z): Calcd. for $\text{C}_{23}\text{H}_{15}\text{N}_4\text{O}_3\text{S}^+$ ($[\text{M} + \text{H}]^+$), 427.0859, found, 427.0852.

6a. White solid. 55.6 mg, 65%. NMR Spectroscopy: ^1H NMR (400 MHz, CDCl_3) δ 8.62–8.58 (m, 3H), 7.75–7.65 (m, 3H), 7.57–7.49 (m, 3H), 7.47–7.42 (m, 1H), 7.34–7.30 (m, 1H), 7.04 (t, $J = 4.8$ Hz, 1H), 2.47 (s, 3H), 2.37 (s, 3H). ^{13}C NMR (100 MHz, CDCl_3) δ 162.0, 157.8, 157.1, 145.4, 135.8, 132.6, 131.5, 129.4, 129.2, 128.1, 125.8, 125.1, 122.3, 121.7, 119.7, 117.5, 117.0, 115.8, 10.6, 8.5. Mass Spectrometry: HRMS (ESI-TOF) (m/z): Calcd. for $\text{C}_{23}\text{H}_{19}\text{N}_4\text{O}_3\text{S}^+$ ($[\text{M} + \text{H}]^+$), 431.1172, found, 431.1181.

6b. White solid. 71.7 mg, 87%. NMR Spectroscopy: ^1H NMR (400 MHz, CDCl_3) δ 7.71 (dd, $J = 6.6$, 2.8 Hz, 2H), 7.57–7.45 (m, 4H), 7.40 (dd, $J = 8.1$, 1.5 Hz, 1H), 7.36 (s, 1H), 3.83 (s, 3H), 3.00–2.93 (m, 1H), 2.24 (s, 3H), 2.17 (s, 3H), 1.28 (s, 3H), 1.26 (s, 3H). ^{13}C NMR (100 MHz, CDCl_3) δ 161.1, 153.3, 151.1, 144.9, 135.1, 132.3, 131.4, 130.0, 129.6, 129.4, 129.2, 128.8, 125.6, 125.1, 61.8, 33.7, 23.7, 14.8, 10.4. Mass Spectrometry: HRMS (ESI-TOF) (m/z): Calcd. for $\text{C}_{22}\text{H}_{25}\text{N}_2\text{O}_4\text{S}^+$ ($[\text{M} + \text{H}]^+$), 413.1530, found, 413.1541.

6c. White solid. 71.2 mg, 75%. NMR Spectroscopy: ^1H NMR (400 MHz, CDCl_3) δ 7.58–7.56 (m, 2H), 7.51–7.34 (m, 11H), 3.85 (s, 3H), 3.02–2.95 (m, 1H), 2.20 (s, 3H), 1.29 (s, 3H), 1.28 (s, 3H). ^{13}C NMR (100 MHz, CDCl_3) δ 160.1, 153.3, 151.1, 144.3, 135.0, 132.6, 131.4, 130.4, 130.3, 130.0, 129.5, 129.5, 129.4, 128.8, 127.3, 125.6, 125.1, 61.9, 3.7, 23.7, 14.8. Mass Spectrometry: HRMS (ESI-TOF) (m/z): Calcd. for $\text{C}_{27}\text{H}_{27}\text{N}_2\text{O}_4\text{S}^+$ ($[\text{M} +$

H⁺), 475.1686, found, 475.1686.

6d. White solid. 69.2 mg, 69%. NMR Spectroscopy: ¹H NMR (400 MHz, CDCl₃) δ 8.39 (d, *J* = 8.5 Hz, 1H), 8.17 (d, *J* = 4.8 Hz, 2H), 8.06 (d, *J* = 7.7 Hz, 4H), 7.64 (t, *J* = 7.4 Hz, 2H), 7.56–7.48 (m, 5H), 7.41 (t, *J* = 7.7 Hz, 1H), 7.28 (d, *J* = 7.5 Hz, 1H), 6.86 (t, *J* = 4.8 Hz, 1H), 1.77 (s, 3H). ¹³C NMR (100 MHz, CDCl₃) δ 157.3, 156.5, 139.3, 135.2, 133.7, 129.8, 128.4, 127.6, 125.7, 123.6, 121.9, 121.3, 119.7, 117.0, 115.1, 9.0. Mass Spectrometry: HRMS (ESI-TOF) (*m/z*): Calcd. for C₂₅H₂₁N₄O₃S₂⁺ ([M + H]⁺), 505.0999, found, 505.1004.

6e. White solid. 97.8 mg, 92%. NMR Spectroscopy: ¹H NMR (400 MHz, CDCl₃) δ 8.37 (d, *J* = 8.5 Hz, 1H), 8.22 (d, *J* = 4.8 Hz, 2H), 7.92 (d, *J* = 8.3 Hz, 4H), 7.55 (d, *J* = 7.8 Hz, 1H), 7.40 (t, *J* = 7.4 Hz, 1H), 7.28–7.25 (m, 5H), 6.87 (t, *J* = 4.8 Hz, 1H), 2.45 (s, 6H), 1.80 (s, 3H). ¹³C NMR (100 MHz, CDCl₃) δ 157.2, 156.6, 144.7, 136.5, 135.1, 129.8, 129.0, 127.6, 125.6, 123.9, 121.8, 121.1, 119.7, 116.9, 115.1, 21.7, 9.1. Mass Spectrometry: HRMS (ESI-TOF) (*m/z*): Calcd. for C₂₇H₂₅N₄O₃S₂⁺ ([M + H]⁺), 533.1312, found, 533.1305.

3. Results and discussion

We commenced our studies by screening the reaction conditions of the coupling between an oxime ether (**1e**) and saccharin **2a** (Table 1). With [Cp*RhCl₂]₂/AgSbF₆ as a catalyst and PhI(OAc)₂ as an oxidant, a coupling occurred in CH₃CN (100 °C) to give the desired product **3e** in 28% yields. Solvent screening revealed that TFE was the best choice, and the yield of **3e** was increased to 75% (Table 1, entry 7). The yield was improved to

Table 1
Optimization studies.^a

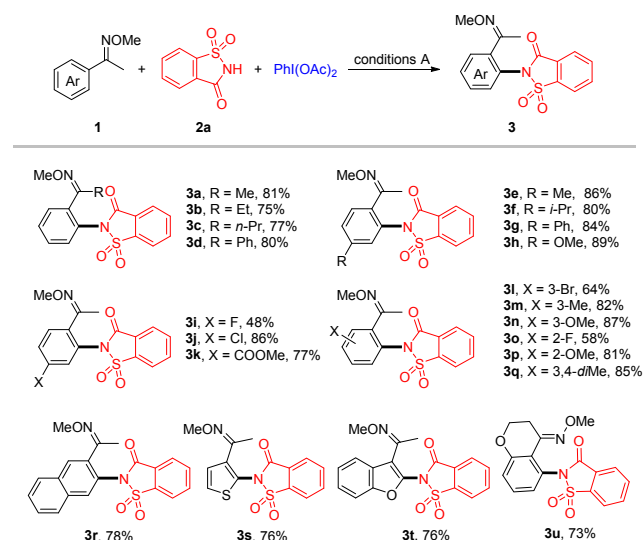
Entry	Catalyst (mol%)	Solvent	Yield ^b (%)
1	[Cp*RhCl ₂] ₂ (4)/AgSbF ₆ (16)	MeCN	28
2	[Cp*RhCl ₂] ₂ (4)/AgSbF ₆ (16)	DCE	<5
3	[Cp*RhCl ₂] ₂ (4)/AgSbF ₆ (16)	THF	n.r.
4	[Cp*RhCl ₂] ₂ (4)/AgSbF ₆ (16)	PhCF ₃	n.r.
5	[Cp*RhCl ₂] ₂ (4)/AgSbF ₆ (16)	acetone	<5
6	[Cp*RhCl ₂] ₂ (4)/AgSbF ₆ (16)	HFIP	37
7	[Cp*RhCl ₂] ₂ (4)/AgSbF ₆ (16)	TFE	75
8	RhCp*(CH ₃ CN) ₃ (SbF ₆) ₂ (8)	TFE	87
9 ^c	RhCp*(CH ₃ CN) ₃ (SbF ₆) ₂ (8)	TFE	<5
10 ^d	RhCp*(CH ₃ CN) ₃ (SbF ₆) ₂ (8)	TFE	83
11	RhCp*(CH ₃ CN) ₃ (SbF ₆) ₂ (5)	TFE	86
12	[Cp*RhCl ₂] ₂ (4)	TFE	61
13	AgSbF ₆ (16)	TFE	0
14	Pd(OAc) ₂ (10)	TFE	0
15	CoCp*(CO) ₂ (10)/AgSbF ₆ (20)	TFE	0
16	Ru(p-cymene) ₂ (SbF ₆) ₂ (5)	TFE	0

^a Reaction conditions: **1e** (0.2 mmol), **2a** (0.3 mmol), PhI(OAc)₂ (0.3 mmol), Rh Catalyst, solvent (2.0 mL) at 100 °C under air for 48 h. ^b Isolated yield after column chromatography (Yields <5% was determined by TLC and conformed by ¹H NMR spectroscopy using 1,3,5-trimethylbenzene as an internal standard). ^c 80 °C. ^d 120 °C.

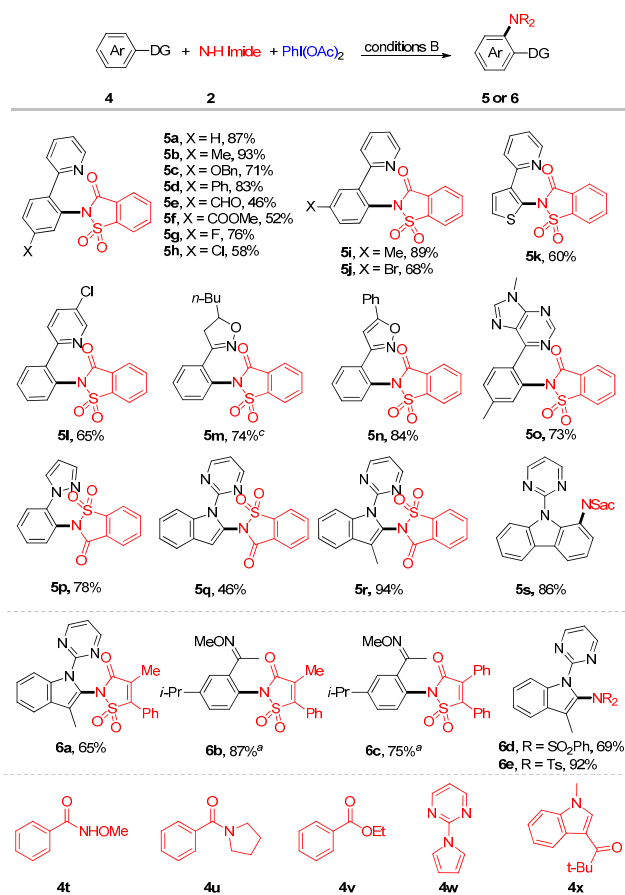
87% when the catalyst was switched to RhCp*(CH₃CN)₃(SbF₆)₂ (Table 1, entry 8). Reactions performed at 80 or 120 °C all lead to lower yields (Table 1, entries 9 and 10). Gratifyingly, the yield of **3e** was essentially unaffected even under lower catalyst loading (5 mol%, entry 11). The rhodium catalyst proved to be indispensable, and no reaction occurred when it was omitted (Table 1, entry 13). Other transition metals such as Pd, Co, or Ru were proved to be inefficient (Table 1, entries 14–16).

With the optimal reaction conditions in hand, we next explored the scope and limitation of this system. As given in Scheme 2, a range of substituted oxime ethers were examined in the coupling with saccharin **2a**. Various substituted *O*-Me oximes readily coupled with **2a** under the standard conditions to afford the imidation products (**3a–3t**) in 48%–89% yields. Different electron-donating, -withdrawing and halogen groups at *para* position of oximes were well tolerated. The reaction also tolerated electron-withdrawing and -donating *meta*-substituents (**1l–1n**) and C–H imidation occurred selectively at the less hindered *ortho* site. Oximes bearing *ortho* OMe and F groups also provide the desired products **3o** and **3p** in moderate yields (58%, 81%). Furthermore, *di*-substituted oxime (**1q**), naphthalene (**1r**) and heterocyclic oxime (**1s**, **1t**) are also viable substrates with good coupling efficiency (76%–85%). Moreover, the oxime substrate was not limited to that of acetophenone, and the reaction proceeded smoothly when the carbon chain in the oxime was elongated (**1b**, **1c**) or when the oxime of benzophenone (**1d**) or a cyclic ketone (**1u**) was used (73%–80%).

The C–H substrate was not restricted to oximes. It was found that the directing group could be smoothly extended to different heterocycles under modified conditions (Conditions B). As shown in Scheme 3, various 2-arylpiperidines bearing a *para* substituent (**5a–5h**) coupled with saccharin in consistently good to high yields, where both electron-donating and -withdrawing groups were tolerated. Introduction of a methyl or bromine group into the *meta* position of benzene ring



Scheme 2. Scope of Coupling of Oxime Ethers with Saccharin. Reaction conditions A: oxime ether (**1**, 0.2 mmol), saccharin (**2a**, 0.3 mmol), RhCp*(CH₃CN)₃(SbF₆)₂ (5 mol %), PhI(OAc)₂ (0.3 mmol), TFE (2.0 mL) at 100 °C under air for 48 h.

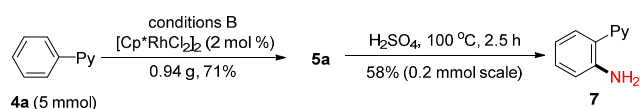


Scheme 3. Scope of coupling of arenes with N-H imides. Conditions B: arene (0.2 mmol), **2** (0.3 mmol), PhI(OAc)₂ (0.3 mmol), [Cp**Rh*Cl₂]₂ (4 mol %), NaOAc (0.06 mmol), TFE (1.0 mL), CH₃CN (1.0 mL) at 100 °C, under air for 48 h. ^aUnder Conditions A.

caused the reaction to occur at the less steric hindered *ortho* site. A thiophene ring was also compatible (**5k**). Other heterocycles such as dihydroisoxazole, isoxazole, pyrazole, purine, and pyrimidine were suitable directing groups (**5m–5s**). Furthermore, the amination source was further extended to other saccharin analogues and to dibenzenesulfonimide derivatives, and the coupled products were isolated in 65%–92% yields (**6a–6e**). Unfortunately, *N*-OMe benzamide (**4t**), phenyl(pyrrrolidin-1-yl)methanone (**4u**), benzoate (**4v**), 2-(1H-pyrrol-1-yl)pyrimidine (**4w**) and 3-pivaloylindole (**4x**) were not suitable for this aminating system.

To demonstrate the synthetic utility of the imidation reaction, a larger-scale (5 mmol) synthesis has been performed for the coupling of 2-phenylpyridine under a reduced catalyst loading, and product **5a** was isolated in 71% yield (Scheme 4). Treatment of **5a** with concentrated H₂SO₄ afforded primary amine **7** [78].

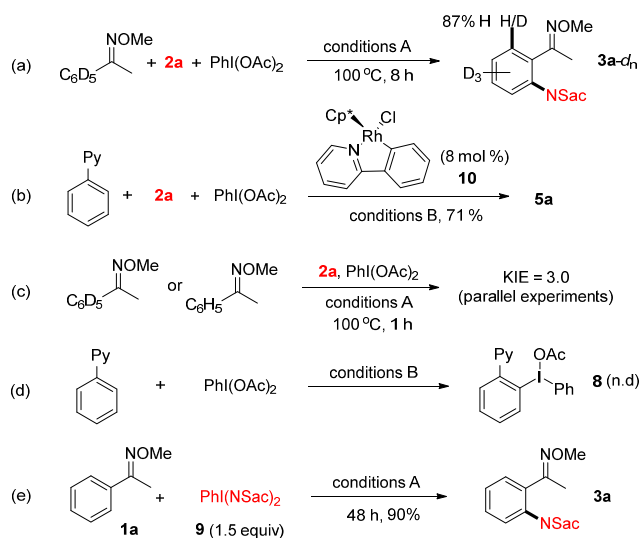
To gain mechanistic insight into this coupling system, several experiments have been conducted and the results are summarized in Scheme 5. The coupling of oxime **1a-d₅** and **2a** under standard conditions afford **3a-d_n** with 87% H/D exchange at the *ortho* position (Scheme 5(a)), suggesting reversibility of C–H activation. As a catalyst precursor, rhodacycle **10** [65]



Scheme 4. Gram-scale synthesis and derivatization.

successfully catalyzed the coupling of **4a** and **2a** to give **5a** in 71% yield, indicated the relevancy of C–H activation. A kinetic isotope effect (KIE) of 3.0 was obtained from parallel experiments using **1a** and **1a-d₅** in the coupling with **2a** at a low conversion under the standard conditions, indicating that C–H bond activation might be involved in the turnover-limiting step. Without NH saccharin, no reaction occurred, indicating the transformation may not processed *via* diaryliodonium salt **8** [85,86]. Furthermore, iodine(III) imido compound **9** was prepared according to the literature report [75], which reacted smoothly with oxime **1a** in comparably high yield. It follows that compound **9** is easily generated under the catalytic conditions from PhI(OAc)₂ and saccharin [75], and this represents rare *in situ* umpolung of the imidating reagent. Though similar work has been reported by DeBoef [77] and co-workers using iodine(III) imido and copper salts, stoichiometric metal was inescapable to achieve high reactivity.

Theoretical calculation was conducted using Gaussian 09 program at the density functional theory level (M11-L) to gain a better understanding of the reaction mechanism. Based on our experimental observation, the species [PhC(CH₃)=NOCH₃]₂Cp**Rh*²⁺ (**Cat.**) was regarded as the starting point in the current systems (Scheme 6). Firstly, the C–H activation occurs via a concerted metalation-deprotonation (CMD) transition state **TS-1** ($\Delta G^\ddagger = 18.4$ kcal/mol) to form a 5-membered rhodacycle intermediate **INT-1** exoergic by 2.3 kcal/mol. This is followed by coordination of O atom in **9** to the Rh center to form **INT-2**. There are two distinct pathways have been taken into account for the cleavage of I–N bond and the formation of C–N bond in complex **INT-2**, namely, oxidation addition/reduction elimination pathway and I–C bond intermediate formation pathway.



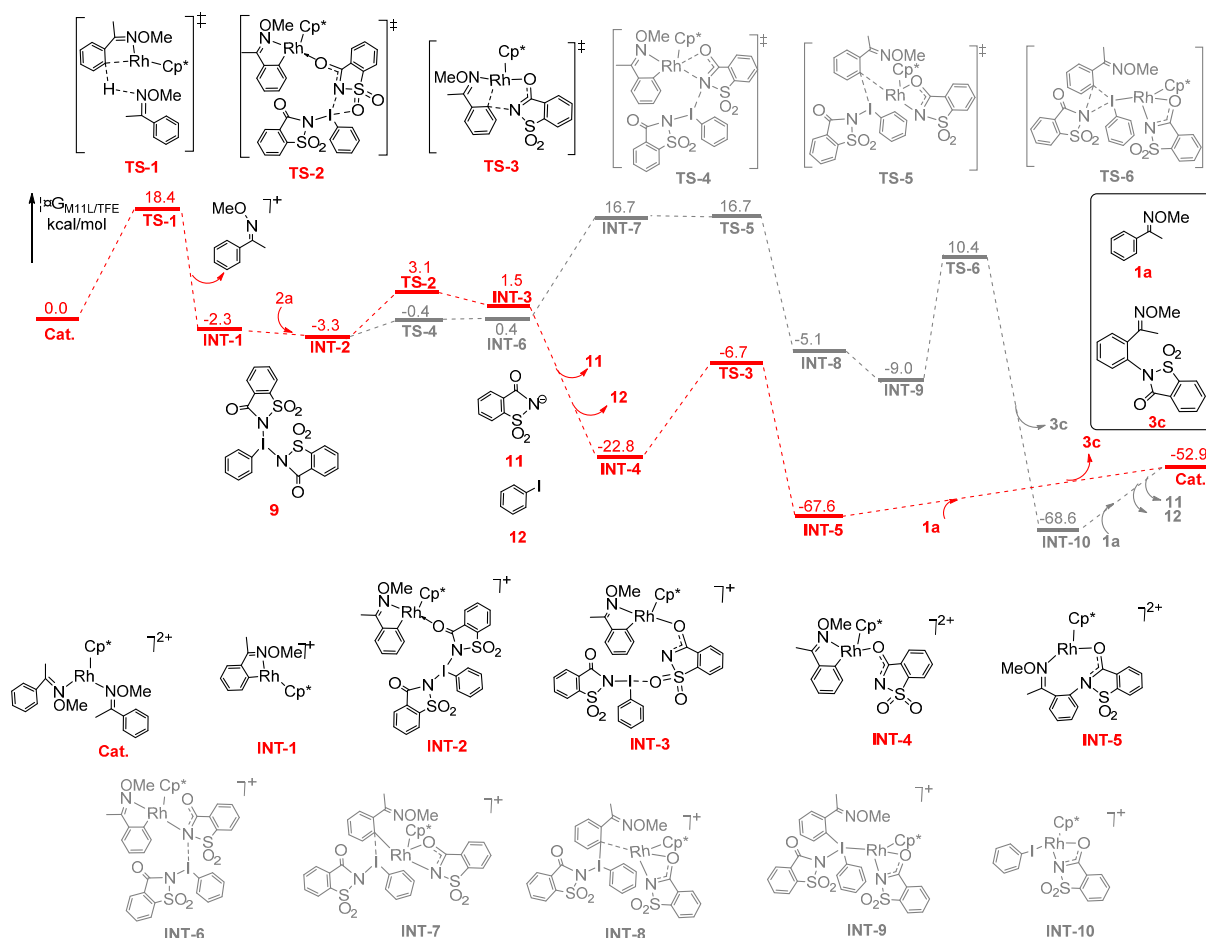
Scheme 5. Mechanistic investigations.

We first computed the feasibility of oxidation addition/reduction elimination pathway. From **INT-2**, with the breaking of I–N bond, a weak I–O bond is forming via a transition state **TS-2** with a barrier of 6.4 kcal/mol, leading to an intermediate **INT-3**. From **INT-2**, **TS-2** to **INT-3**, the I–N distances are increased from 2.43, 2.82 to 3.60 Å, whereas the I–O distance are decreased from 4.52, 3.00 to 2.47 Å, respectively. Thereafter, accompanied with the broken of the weak I–O bond, a stable high-valent Rh(V) intermediate **INT-4** is formed by release of **11** and **12**, which is exergonic by 24.3 kcal/mol. The Rh(V) species **INT-4** then undergoes reduction elimination (via **TS-3** with a barrier of 16.1 kcal/mol) to produce **INT-5**, which upon formation of C–N bond leads to the final product **3c** and realizes the regeneration of catalyst. The barrier for reduction elimination is 16.1 kcal/mol and the whole process is extremely exergonic by 52.9 kcal/mol.

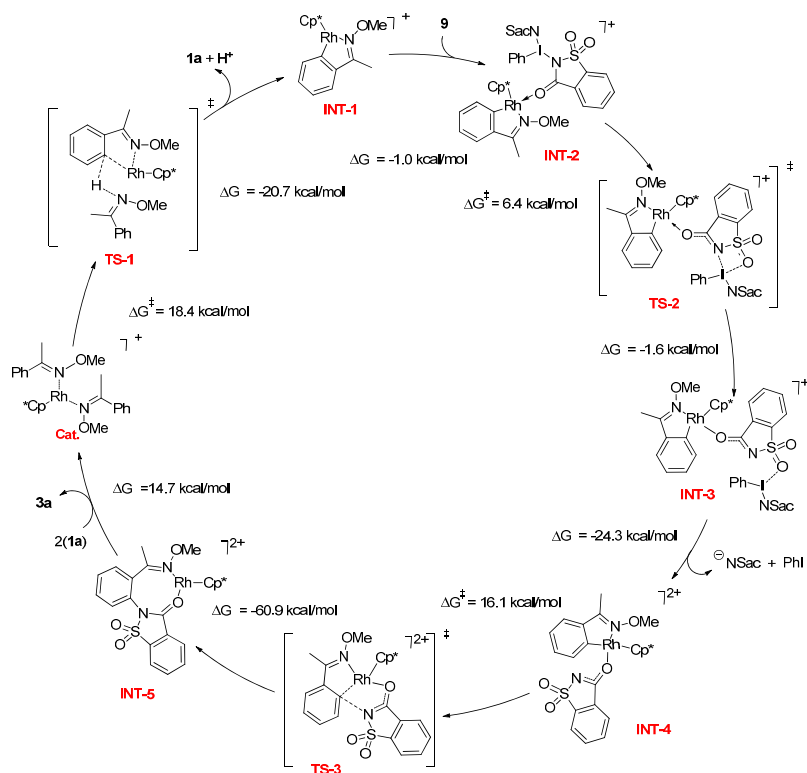
Different from the oxidation addition/reduction elimination pathway, we also consider another pathway for formation of C–N bond final product, in which an I–C bond intermediate is formed. From **INT-2**, rather than formation of I–O bond, with the breaking of I–N bond, a Rh–N bond is forming via a transition state **TS-4** with a barrier of 2.9 kcal/mol, leading to an intermediate **INT-6**. Then, accompanied with the dissociation of N(OMe)–Rh bond, **INT-6** can isomerize into **INT-7** by rotation of the C–C single bond endergonically by 16.3 kcal/mol.

Subsequently, through **TS-5** with a barrier of 20.0 kcal/mol, in which the C–Rh bond is breaking and the I–C bond is forming, an I–C bond intermediate **INT-8** formed. From **INT-7**, **TS-4** to **INT-8**, the Rh–C distances are increased from 2.06, 2.14 to 3.07 Å, whereas the I–C distance are decreased from 2.93, 2.64 to 2.19 Å, respectively. Thereafter, the I atom of the dissociated I moiety is closing to the Rh atom of the dissociated Rh moiety, which leads to an I–Rh bond intermediate **INT-9**. Accompanied with the broken of I–C bond and the formation of a new C–N bond via **TS-6** with a barrier of 19.4 kcal/mol, an intermediate **INT-10** formed by release of the final product **3c**. Finally, the dissociation of **11** and **12** could lead to the regeneration of catalyst. Based on the above studies, the oxidation addition/reduction elimination pathway is significantly more favored than the I–C intermediate formation pathway, due to it requires to overcome lower barrier (16.1 vs 20.0 kcal/mol). Moreover, our calculation shown that the C–H activation is the rate-determining step.

A plausible catalytic cycle is proposed on the basis of our experimental results and our DFT calculations (Scheme 7). Starting from an oxime coordinated Cp*Rh(III) catalyst, cyclometalation of **1a** via CMD mechanism gives a rhodacyclic intermediate **INT-1** with 18.4 kcal/mol barrier. Interactions of **INT-1** and the active imidating reagent **9** renders elongation of the N–I bond with concurrent formation of a weak O–I bond,



Scheme 6. Theoretical calculation on the possible reaction pathways.



Scheme 7. Proposed pathway of C–H imidation.

leading to formation of an O-bound intermediate **Int-3** with a low activation barrier (6.4 kcal/mol). Subsequent oxidative Rh–O bond formation with displacement of the PhI and saccharin co-products produces a Rh(V) [87–97] species **Int-4**. C–N reductive elimination of **Int-4** was calculated to occur via a five-membered ring transition state at an activation free energy of 16.1 kcal/mol. Dissociation of the coupling product **3a** regenerates the active catalyst for the next cycle.

4. Conclusions

In summary, we have realized Rh(III)-catalyzed oxidative C–H imidation of arenes with saccharin using PhI(OAc)₂ as an environmentally benign oxidant avoiding stoichiometric metal complexes. This transformation provided efficient synthesis of tertiary amines under operationally simple conditions and exhibited a broad substrate scope with good functional tolerance. DFT studies suggest that the C–N coupling occurs via a Rh(III)–Rh(V)–Rh(III) cycle.

References

- [1] R. Hili, A. K. Yudin, *Nat. Chem. Biol.*, **2006**, 2, 284–287.
- [2] C. Sánchez, C. Méndez, J. A. Salas, *Nat. Prod. Rep.*, **2006**, 23, 1007–1045.
- [3] A. Ricci, *Amino Group Chemistry, From Synthesis to the Life Sciences*, Wiley-VCH, Weinheim, **2007**.
- [4] J. Yamaguchi, A. D. Yamaguchi, K. Itami, *Angew. Chem. Int. Ed.*, **2012**, 51, 8960–9009.
- [5] J. Kim, M. Movassaghi, *Acc. Chem. Res.*, **2015**, 48, 1159–1171.
- [6] T. E. Miller, M. Beller, *Chem. Rev.*, **1998**, 98, 675–704.
- [7] J. F. Hartwig, *Acc. Chem. Res.*, **2008**, 41, 1534–1544.
- [8] D. S. Surry, S. L. Buchwald, *Angew. Chem. Int. Ed.*, **2008**, 47, 6338–6361.
- [9] J. Bariwal, E. Van der Eycken, *Chem. Soc. Rev.*, **2013**, 42, 9283–9303.
- [10] F. Paul, J. Patt, J. F. Hartwig, *J. Am. Chem. Soc.*, **1994**, 116, 5969–5970.
- [11] A. S. Guram, S. L. Buchwald, *J. Am. Chem. Soc.*, **1994**, 116, 7901–7902.
- [12] P. Y. S. Lam, G. Vincent, C. G. Clark, S. Deudon, P. K. Jadhav, *Tetrahedron Lett.*, **2001**, 42, 3415–3418.
- [13] K. Sanjeeva Rao, T.-S. Wu, *Tetrahedron*, **2012**, 68, 7735–7754.
- [14] F. Ullmann, *Ber. Dtsch. Chem. Ges.*, **1903**, 36, 2382–2384.
- [15] J. Niu, H. Zhou, Z. Li, J. Xu, S. Hu, *J. Org. Chem.*, **2008**, 73, 7814–7817.
- [16] W. Zhou, M. Fan, J. Yin, Y. Jiang, D. Ma, *J. Am. Chem. Soc.*, **2015**, 137, 11942–11945.
- [17] J. Gao, S. Bhunia, K. Wang, L. Gan, S. Xia, D. Ma, *Org. Lett.*, **2017**, 19, 2809–2812.
- [18] T. Xiong, Q. Zhang, *Chem. Soc. Rev.*, **2016**, 45, 3069–3087.
- [19] H. Xu, X. Qiao, S. Yang, Z. Shen, *J. Org. Chem.*, **2014**, 79, 4414–4422.
- [20] J. Hu, X. Zuo, H. Huang, *Chin. J. Catal.*, **2013**, 34, 1644–1650.
- [21] K. Sun, Y. Li, T. Xiong, J. Zhang, Q. Zhang, *J. Am. Chem. Soc.*, **2011**, 133, 1694–1697.
- [22] E. J. Yoo, S. Ma, T.-S. Mei, K. S. L. Chan, J.-Q. Yu, *J. Am. Chem. Soc.*, **2011**, 133, 7652–7655.
- [23] M. Anand, R. B. Sunoj, H. F. Schaefer, *J. Am. Chem. Soc.*, **2014**, 136, 5535–5538.
- [24] V. S. Thirunavukkarasu, S. I. Kozhushkov, L. Ackermann, *Chem. Commun.*, **2014**, 50, 29–39.
- [25] K. Raghuvanshi, D. Zell, K. Rauch, L. Ackermann, *ACS Catal.*, **2016**, 6, 3172–3175.
- [26] M. Moselage, J. Li, L. Ackermann, *ACS Catal.*, **2016**, 6, 498–525.

Graphical Abstract

Chin. J. Catal., 2020, 41: 1723–1733 doi: 10.1016/S1872-2067(20)63587-2

Rhodium(III)-catalyzed chelation-assisted C–H imidation of arenes via umpolung of the imidating reagent

Guangfan Zheng, Jiaqiong Sun, Youwei Xu, Xukai Zhou, Hui Gao*, Xingwei Li*
 Shaanxi Normal University; Guangzhou Medical University;
 Dalian Institute of Chemical Physics, Chinese Academy of Sciences

Rh(III)-catalyzed oxidative C–H imidation of arenes has been realized via umpolung of saccharin using $\text{PhI}(\text{OAc})_2$ as an oxidant. The reaction features a wide scope of substrate and operational simplicity. DFT studies suggest that the C–N coupling occurs via a Rh(III)–Rh(V)–Rh(III) cycle.



- Direct C–H/N–H oxidative coupling
- *in situ* generated I(III) imido reagent
- 45 examples; up to 93% yields
- DFT studies; Rh(V) intermediate

- [27] M.-L. Louillat, F. W. Patureau, *Chem. Soc. Rev.*, **2014**, 43, 901–910.
- [28] J. Jiao, K. Murakami, K. Itami, *ACS Catal.*, **2015**, 6, 610–633.
- [29] H. Kim, S. Chang, *ACS Catal.*, **2016**, 6, 2341–2351.
- [30] H. Kim, S. Chang, *Acc. Chem. Res.*, **2017**, 50, 482–486.
- [31] Y. Park, Y. Kim, S. Chang, *Chem. Rev.*, **2017**, 117, 9247–9301.
- [32] D. A. Colby, R. G. Bergman, J. A. Ellman, *Chem. Rev.*, **2010**, 110, 624–655.
- [33] T. Satoh, M. Miura, *Chem.-Eur. J.*, **2010**, 16, 11212–11222.
- [34] D. A. Colby, A. S. Tsai, R. G. Bergman, J. A. Ellman, *Acc. Chem. Res.*, **2012**, 45, 814–825.
- [35] G. Song, F. Wang, X. Li, *Chem. Soc. Rev.*, **2012**, 41, 3651–3678.
- [36] F. W. Patureau, J. Wencel-Delord, F. Glorius, *Aldrichim. Acta.*, **2012**, 45, 31–44.
- [37] N. Kuhl, N. Schroder, F. Glorius, *Adv. Synth. Catal.*, **2014**, 356, 1443–1460.
- [38] G. Song, X. Li, *Acc. Chem. Res.*, **2015**, 48, 1007–1020.
- [39] W. Dai, Y. Liu, T. Tong, X. Li, F. Luo, *Chin. J. Catal.*, **2014**, 35, 1012–1016.
- [40] J. Y. Kim, S. H. Park, J. Ryu, S. H. Cho, S. H. Kim, S. Chang, *J. Am. Chem. Soc.*, **2012**, 134, 9110–9113.
- [41] J. Ryu, K. Shin, S. H. Park, J. Y. Kim, S. Chang, *Angew. Chem., Int. Ed.*, **2012**, 51, 9904–9908.
- [42] D. G. Yu, M. Suri, F. Glorius, *J. Am. Chem. Soc.*, **2013**, 135, 8802–8805.
- [43] Y. Lian, J. R. Hummel, R. G. Bergman, J. A. Ellman, *J. Am. Chem. Soc.*, **2013**, 135, 12548–12551.
- [44] K. Shin, Y. Baek, S. Chang, *Angew. Chem. Int. Ed.*, **2013**, 52, 8031–8036.
- [45] S. H. Park, J. Kwak, K. Shin, J. Ryu, Y. Park, S. Chang, *J. Am. Chem. Soc.*, **2014**, 136, 2492–2502.
- [46] Y. Park, K. T. Park, J. G. Kim, S. Chang, *J. Am. Chem. Soc.*, **2015**, 137, 4534–4542.
- [47] H. Wang, G. Tang, X. Li, *Angew. Chem. Int. Ed.*, **2015**, 54, 13049–13052.
- [48] M. A. Ali, X. Yao, G. Li, H. Lu, *Org. Lett.*, **2016**, 18, 1386–1389.
- [49] Q. Wang, X. Li, *Org. Lett.*, **2016**, 18, 2102–2105.
- [50] J. Wang, S. Zha, K. Chen, F. Zhang, C. Song, J. Zhu, *Org. Lett.*, **2016**, 18, 2062–2065.
- [51] Q. Wang, F. Wang, X. Yang, X. Zhou, X. Li, *Org. Lett.*, **2016**, 18, 6144–6147.
- [52] F. Wang, L. Jin, L. Kong, X. Li, *Org. Lett.*, **2017**, 19, 1812–1815.
- [53] S. Yu, G. Tang, Y. Li, X. Zhou, Y. Lan, X. Li, *Angew. Chem. Int. Ed.*, **2016**, 55, 8696–8700.
- [54] L. Shi, B. Wang, *Org. Lett.*, **2016**, 18, 2820–2823.
- [55] C. Grohmann, H. G. Wang, F. Glorius, *Org. Lett.*, **2012**, 14, 656–659.
- [56] K.-H. Ng, Z. Zhou, W.-Y. Yu, *Org. Lett.*, **2012**, 14, 272–275.
- [57] R.-J. Tang, C.-P. Luo, L. Yang, C.-J. Li, *Adv. Synth. Catal.*, **2013**, 355, 869–873.
- [58] F.-N. Ng, Z. Y. Zhou, W.-Y. Yu, *Chem. Eur. J.*, **2014**, 20, 4474–4480.
- [59] C. Grohmann, H. Wang, F. Glorius, *Org. Lett.*, **2013**, 15, 3014–3017.
- [60] B. J. Zhou, J. Du, Y. X. Yang, H. J. Feng, Y. C. Li, *Org. Lett.*, **2014**, 16, 592–595.
- [61] K. Wu, Z. L. Fan, Y. Xue, Q. Z. Yao, A. Zhang, *Org. Lett.*, **2014**, 16, 42–45.
- [62] G. Ju, G. Li, G. Qian, J. Zhang, Y. Zhao, *Org. Lett.*, **2019**, 21, 7333–7336.
- [63] W. Yang, J. Q. Sun, X. X. Xu, Q. Zhang, Q. Liu, *Chem. Commun.*, **2014**, 50, 4420–4422.
- [64] B. Zhou, J. Du, Y. Yang, H. Feng, Y. Li, *Org. Lett.*, **2013**, 15, 6302–6305.
- [65] F. Xie, Z. Qi, X. Li, *Angew. Chem. Int. Ed.*, **2013**, 52, 11862–11866.
- [66] X. H. Hu, X. F. Yang, T. P. Loh, *ACS Catal.*, **2016**, 6, 5930–5934.
- [67] H. Zhao, Y. Shang, W. Su, *Org. Lett.*, **2013**, 15, 5106–5109.
- [68] H. Kim, K. Shin, S. Chang, *J. Am. Chem. Soc.*, **2014**, 136, 5904–5907.
- [69] H. Kim, S. Chang, *ACS Catal.*, **2015**, 5, 6665–6669.
- [70] H. W. Wang, Y. Lu, B. Zhang, J. He, H. J. Xu, Y. S. Kang, W. Y. Sun, J. Q. Yu, *Angew. Chem. Int. Ed.*, **2017**, 56, 7449–7453.
- [71] A. Yoshimura, V. V. Zhdankin, *Chem. Rev.*, **2016**, 116, 3328–3435.
- [72] J. A. Souto, D. Zian, K. Muñiz, *J. Am. Chem. Soc.*, **2012**, 134, 7242–7245.
- [73] J. A. Souto, P. Becker, A. Iglesias, K. Muñiz, *J. Am. Chem. Soc.*, **2012**, 134, 15505–15511.
- [74] J. A. Souto, C. Martínez, I. Vellilla, K. Muñiz, *Angew. Chem. Int. Ed.*, **2013**, 52, 1324–1328.
- [75] A. Yoshimura, S. R. Koski, J. M. Fuchs, A. Saito, V. N. Nemykin, V. V. Zhdankin, *Chem.-Eur. J.*, **2015**, 21, 5328–5331.
- [76] A. Pialat, J. Bergès, A. Sabourin, R. Vinck, B. Liégault, M. Taillefer, *Chem.-Eur. J.*, **2015**, 21, 10014–10018.
- [77] A. A. Kantak, L. Marchetti, B. DeBoef, *Chem. Commun.*, **2015**, 51, 3574–3577.
- [78] K. Kiyokawa, T. Kosaka, T. Kojima, S. Minakata, *Angew. Chem. Int. Ed.*, **2015**, 54, 13719–13723.
- [79] Y. K. Liu, S. J. Lou, D. Q. Xu, Z. Y. Xu, *Chem.-Eur. J.*, **2010**, 16, 13590–13593.

- [80] I. Cerna, R. Pohl, B. Klepetarova, M. Hocek, *J. Org. Chem.*, **2008**, 73, 9048–9054.
- [81] H. Kim, J. Park, J. G. Kim, S. Chang, *Org. Lett.*, **2014**, 16, 5466–5469.
- [82] J. A. Leitch, C. L. McMullin, M. F. Mahon, Y. Bhonoah, C. G. Frost, *ACS Catal.*, **2017**, 7, 2616–2623.
- [83] B. Schulze, G. Kirsten, S. Kirrbach, A. Rahm, H. Heimgartner, *Helvet. Chim. Acta*, **1991**, 74, 1059–1070.
- [84] L. Song, L. Zhang, S. Luo, J. P. Cheng, *Chem.-Eur. J.*, **2014**, 20, 14231–14234.
- [85] F. Xie, Z. Zhang, X. Yu, G. Tang, X. Li, *Angew. Chem. Int. Ed.*, **2015**, 54, 7405–7409.
- [86] F. Wang, X. Yu, Z. Qi, X. Li, *Chem.-Eur. J.*, **2016**, 22, 511–516.
- [87] L. Xu, Q. Zhu, G. Huang, B. Cheng, Y. Xia, *J. Org. Chem.*, **2012**, 77, 3017–3024.
- [88] F. Xie, Z. Qi, S. Yu, X. Li, *J. Am. Chem. Soc.*, **2014**, 136, 4780–4787.
- [89] C. R. Turlington, J. Morris, P. S. White, W. W. Brennessel, W. D. Jones, M. Brookhart, J. L. Templeton, *Organometallics*, **2014**, 33, 4442–4448.
- [90] T. Zhou, W. Guo, Y. Xia, *Chem.-Eur. J.*, **2015**, 21, 9209–9218.
- [91] W. Guo, Y. Xia, *J. Org. Chem.*, **2015**, 80, 8113–8121.
- [92] W. Ai, Y. Wu, H. Tang, X. Yang, Y. Yang, Y. Li, B. Zhou, *Chem. Commun.*, **2015**, 51, 7871–7874.
- [93] J. Li, Z. Qiu, *J. Org. Chem.*, **2015**, 80, 10686–10693.
- [94] J. Chen, W. Guo, Y. Xia, *J. Org. Chem.*, **2016**, 81, 2635–2638.
- [95] J.-Q. Wu, S.-S. Zhang, H. Gao, Z. Qi, C.-J. Zhou, W.-W. Ji, Y. Liu, Y. Chen, Q. Li, X. Li, H. Wang, *J. Am. Chem. Soc.*, **2017**, 139, 3537–3545.
- [96] X. G. Liu, H. Gao, S. S. Zhang, Q. Li, H. Wang, *ACS Catal.*, **2017**, 7, 5078–5086.
- [97] S. Vázquez-Céspedes, X. Wang, F. Glorius, *ACS Catal.*, **2018**, 8, 242–257.

Rh(III)催化基于胺化试剂极性翻转策略的定位基辅助芳烃C–H键胺化反应

郑光范^{a,c}, 孙佳琼^a, 许有伟^c, 周旭凯^a, 高 辉^{b,#}, 李兴伟^{a,c,*}

^a陕西师范大学化学化工学院, 胶体与界面化学教育部重点实验室, 陕西西安710062

^b广州医科大学药学院&第五附属医院, 分子靶向与临床药理学重点实验室, 广东广州511436

^c中国科学院大连化学物理研究所, 辽宁大连116023

摘要: 芳胺类化合物广泛存在于农药、医药和生物活性分子中, 因此发展芳胺类化合物新的合成方法受到有机合成工作者的广泛关注. Buchwald-Hartwig偶联, Chan-Lam胺化和Ullmann反应等的发展为芳胺类化合物的合成提供了重要方法. 过渡金属催化的C–H键直接胺化反应因起始原料简单易得、高原子和步骤经济性等优势成为合成芳胺类化合物的重要方法. Cp*Rh(III)/Ir(III)等催化的C–H键直接胺化反应有了快速的发展, 合成了大量重要的芳胺类化合物, 但是该类反应局限于应用乃春形式的氮源或预官能化的亲电性胺化试剂, 基于亲核性氮源实现的C–H键胺化反应报道罕见. Su和Chang课题组实现了以TsNH₂为乃春前体的C–H键胺化反应. 近期Yu课题组实现了铑催化当量碳酸银为氧化剂的二级胺类化合物氧化胺化反应. 发展铑催化无需当量金属氧化剂的二级胺类化合物氧化胺化反应值得期待. 我们认为, 通过亲核性胺化试剂极性翻转策略将有望实现该类转化. 高价碘化合物因环境友好和易于操作等优势在C–N键构建领域有着重要应用. 我们认为, 亲核性氮源与醋酸碘苯作用生成高价N–I(III)物种, 可实现极性翻转, 原位生成高活性亲电胺化试剂, 进而在铑催化下实现芳基C–H键的氧化胺化反应.

本文选用糖精衍生物和双苯磺酰亚胺为亲核性氮源, 商业易得、环境友好的醋酸碘苯为氧化剂, 采用胺化试剂极性翻转策略, 实现了定位基辅助的芳基C–H键直接胺化反应. 该策略底物适用范围广泛, 基团的相容性良好, 各种邻间对位取代和双取代的芳烃, 萘环, 噻吩和苯并呋喃, 吡啶, 咪唑等杂环芳烃均可以很好的发生反应. 该反应可扩展至脲醚和吡啶, 嘧啶, 恶唑, 吡唑和嘌呤等氮定位基. 本文完成了45个不同官能团取代的芳胺类化合物的合成, 反应均可以以中等到较高的产率得到目标产物, 且该反应适用于克级规模制备. 该反应条件温和, 操作简单, 为三级芳酰胺类化合物的合成提供了新方法. DFT计算结果表明C–N键的构建过程经历Rh(III)-Rh(V)-Rh(III)催化循环.

关键词: 芳胺; Rh(III)催化; C–H键氧化胺化; 高价碘试剂; 极性翻转

收稿日期: 2020-02-27. 接受日期: 2020-03-30. 出版日期: 2020-11-05.

*通讯联系人. 电话: (029)85318783; 电子信箱: lixw@snnu.edu.cn

#通讯联系人. 电子信箱: gaoh9@gzhu.edu.cn

基金来源: 国家自然科学基金(21525208); 中国博士后基金(2019TQ0192, 2019M653531, 2019M663613); 中央高校基本科研业务费专项资金(GK201903028)和陕西师范大学.

本文的电子版全文由Elsevier出版社在ScienceDirect上出版(<http://www.sciencedirect.com/science/journal/18722067>).